Biochimica et Biophysica Acta 1807 (2011) 391–403

Contents lists available at ScienceDirect

Biochimica et Biophysica Acta

journal homepage: www.elsevier.com/locate/bbabio

Characterization of photosystem II in transgenic tobacco plants with decreased iron superoxide dismutase

Yan Zhang, Shunhua Ding, Qingtao Lu, Zhipan Yang, Xiaogang Wen, Lixin Zhang, Congming Lu *

Photosynthesis Research Center, Key Laboratory of Photobiology, Institute of Botany, Chinese Academy of Sciences, Beijing 100093, PR China

ARTICLE INFO

Article history:
Received 26 October 2010
Received in revised form 7 January 2011
Accepted 14 January 2011
Available online 20 January 2011

Keywords:
Chlorophyll fluorescence
Iron superoxide dismutase
Photosystem II
Photoinhibition
Transformed tobacco (*Nicotiana tabacum*)
Thermoluminescence

ABSTRACT

Iron superoxide dismutases (FeSODs) play an important role in preventing the oxidative damage associated with photosynthesis. To investigate the mechanisms of FeSOD in protection against photooxidative stress, we obtained transgenic tobacco (*Nicotiana tabacum*) plants with severely decreased FeSOD by using a gene encoding tobacco chloroplastic FeSOD for the RNAi construct. Transgenic plants were highly sensitive to photooxidative stress and accumulated increased levels of $O_2^{\bullet-}$ under normal light conditions. Spectroscopic analysis and electron transport measurements showed that PSII activity was significantly reduced in transgenic plants. Flash-induced fluorescence relaxation and thermoluminescence measurements revealed that there was a slow electron transfer between Q_A and Q_B and decreased redox potential of Q_B in transgenic plants, whereas the donor side function of PSII was not affected. Immunoblot and blue native gel analyses showed that PSII protein accumulation was also decreased in transgenic plants. PSII photodamage and D1 protein degradation under high light treatment was increased in transgenic plants, whereas the PSII repair was not affected, indicating that the stability of the PSII complex was decreased in transgenic plants. The results in this study suggest that FeSOD plays an important role in maintaining PSII function by stabilizing PSII complexes in tobacco plants.

1. Introduction

For photosynthetic blue-green algae and higher plants, various reactive oxygen species (ROS), such as the superoxide anion ($O_2^{\bullet-}$), hydrogen peroxide (H_2O_2), hydroxyl radical ($HO^{\bullet}$), are inevitable by-products of photosynthesis even under normal light conditions. When the absorption of light energy exceeds its utilization in photosynthesis, production of ROS is dramatically enhanced. It is generally thought that ROS are involved in light-induced decline of photosynthetic activity termed as 'photoinhibition' [1]. Photosystem II (PSII) complex, in particular, the PSII reaction center D1 protein, is the main target of photoinhibition. ROS can induce the specific cleavage of the D1 protein in vitro [2–6]. Based on in vivo studies of cyanobacteria, it has been suggested that ROS act primarily by inhibiting the synthesis of the D1 protein and not by damaging PSII directly [7–9].

ROS is detoxified via both enzymatic and non-enzymatic mechanisms. Superoxide dismutases (SODs) constitute the first line of defense against $O_2^{\bullet-}$ by rapidly converting $O_2^{\bullet-}$ to H_2O_2 and O_2 [10]. In chloroplasts, there are two types of SOD isozymes, iron SOD (FeSOD) and copper–zinc SOD (Cu/ZnSOD). Comparison of deduced amino acid sequences from the two types of SODs suggests that FeSOD has no sequence similarity to Cu/ZnSODs and probably has evolved separately in eukaryotes [11]. In addition, the functions of FeSODs are specific: the induction of chloroplastic Cu/ZnSOD has been observed in *fsd Arabidopsis* mutant, whereas the induction cannot compensate for the mutation and cannot reverse the phenotype [12]. This functional specialization of FeSODs may be related to their different localizations in the chloroplast [12]. Chloroplastic Cu/ZnSOD is thought to be attached to the thylakoid membranes at the vicinity of photosystem I (PSI) [13,14]. Although FeSODs are attached to the stromal side of the thylakoid membranes [12,15], their subplastidial localization may be different. Immunoblot analysis shows the presence of a FeSOD in the PSII membrane in wheat chloroplasts [16]. FeSODs from *Arabidopsis* and mustard are identified as components of the plastid-encoded polymerase (PEP) complex and are located at thylakoid membrane-associated nucleoids in plastids [12,17,18].

Indeed, there are several lines of evidence suggesting that FeSODs play important roles in protecting chloroplasts from photooxidative damage. Exposure to high light stress results in an increase in FeSOD transcripts in *Arabidopsis* [12]. Proteomic analysis of the response of *Arabidopsis* to high light also revealed that FeSODs are up-regulated [19]. Moreover, knockout FeSOD *Arabidopsis* plants show a typical photooxidative stress symptom even at non-photoinhibitory conditions, as manifested by pale green phenotypes and suppressed growth and abnormal chloroplasts [12]. However, it has been reported that little protection from photoinhibition was observed for overexpression of FeSOD in tobacco [15] or in poplars [20]. This little protective effect may be due to the following reasons: (1) the localization of overexpressed

* Corresponding author. Tel./fax: +86 10 62595516.
E-mail address: lucm@ibcas.ac.cn (C. Lu).

0005-2728/$ – see front matter © 2011 Elsevier B.V. All rights reserved.
doi:10.1016/j.bbabio.2011.01.006

FeSOD may be different from membrane-attached chloroplastic SOD, resulting in a failure of overexpressed FeSOD to be accessible to $O_2^{\bullet-}$ produced in PSI or PSII and to protect chloroplasts from photoinhibition [15,20]; and (2) the overexpression of FeSOD may result in a more rapid production of H_2O_2, which can be equally damaging [15].

In addition to chloroplastic Cu/ZnSOD and FeSOD, non-heme iron and heme-iron of cyt b_{559} have been considered to exhibit superoxide dismutase activity [21,22]. The intermediate potential (IP) form of cyt b_{559} serves as superoxide oxidase that catalyze $O_2^{\bullet-}$ to O_2, and the reduced high potential (HP^{red}) form acts as superoxide reductase to catalyze $O_2^{\bullet-}$ to H_2O_2 [22].

Although it has been shown that FeSOD plays an important role in chloroplast development [12], it is unknown if and how FeSODs protect PSII against photooxidative stress. In addition, the role of increased chloroplastical $O_2^{\bullet-}$ in photoinhibition has not been investigated in vivo. To address the above questions, we generated transgenic tobacco plants with severely decreased chloroplastic FeSOD by the RNA interference technique (RNAi). Our results suggest that FeSOD plays an important role in maintaining the stability of PSII complex and high levels of $O_2^{\bullet-}$ accumulated in transgenic plants result in accelerated PSII photodamage and increased D1 degradation.

2. Materials and methods

2.1. Vectors and plant transformation

The partial coding region for tobacco FeSOD gene (A09032, gi: 411893) was cloned into pKANNIBAL vector between the *Xho*I–*Kpn*I sites in sense orientation and the *Cla*I–*Xba*I sites in antisense orientation [23]. The primers used were: 5′-AAA CTC GAG ATT TGA ACT CCA GCC TCC-3′ and 5′-ATA GGT ACC GAC ACG AGC TTC TCC ATA-3′ (iFSD sense primers) and 5′-TA TCT AGA ATT TGA ACT CCA GCC TCC-3′ and 5′-TAG ATC GAT GAC ACG AGC TTC TCC ATA-3′ (iFSD antisense primers). Construct made in pKANNIBAL was subcloned as *Not*I fragment into pART27, then introduced into *Agrobacterium tumefaciens* strain LBA4404 by tri-parental mating [24]. *Nicotiana tabacum* (Wisconsin 38) were transformed by the standard *Agrobacterium*-mediated transformation [25]. Regenerated plants were transplanted into sterilized soil and grown in a greenhouse at 27/20 °C (day/night), with maximum PPFD of 1000 μmol m^{-2} s^{-1}, and a photoperiod of 12/12-h light/dark.

2.2. Plant materials and growth conditions

The independent transgenic lines were screened by Southern blot and immunoblot analyses. Three independent lines of transgenic tobacco plants (i4, i29, and i34) were selected in the present study. The seeds of these transgenic lines were allowed to germinate on agar in the presence of 50 μg l^{-1} kanamycin. After growth for 2 weeks, plants were transferred to vermiculite which was soaked with Hoagland solution. The transplanted plants were then grown for 2 weeks in a growth chamber at 25 ± 1 °C with PPFD of 100 or alternatively 20 μmol m^{-2} s^{-1}, a relative humidity of 75–80%, and a photoperiod of 12/12-h light/dark. Unless otherwise stated, tobacco plants grown under normal light conditions (100 μmol m^{-2} s^{-1}) were used for most experiments. All the measurements on physiological and biochemical parameters were carried out on the second leaves from the top.

2.3. RT-PCR and real-time RT-PCR

Total RNA was extracted from 0.1-g fresh leaves using the Trizol reagent (Invitrogen Carlsbad, USA). After DNase I treatment to remove any residual genomic DNA contamination, 2 μg of total RNA from each sample was used to synthesize first-strand cDNA in a 20-μl total volume (SuperScript Pre-amplification System, Promega, USA). RT-PCR was performed using the iFSD sense primers and amplified PCR products were collected and analyzed following different numbers (25 cycles, 30 cycles) of amplification cycles. The expression level of tobacco actin was used as an internal control as described previously [26].

The real-time RT-PCR reactions were performed using TaKaRa SYBR Premix ExTaq in an Mx3000P real-time PCR instrument (Stratagene). The amplification of actin was used as an internal control for normalization. The primers for analysis of FeSOD transcript levels were: sense, 5′-ATCAATGAAGCCCAACGG-3′ and antisense, 5′-GCCCAACCAGAGCCAAAT-3′.

2.4. SOD activity gels

Tobacco leaves (0.1 g) were homogenized in 200 μl extraction buffer (100 mM Tris–HCl, pH 8.3, 10 mM $MgCl_2$, 1.0 mM EDTA, 1.0 mM PMSF, 2% (w/v) PVP) and the homogenate was centrifuged at 12,000 × *g* at 4 °C for 10 min. Total protein (80 μg) was separated on 15% nondenaturing polyacrylamide gel in Tris–Gly buffer (pH 8.3) at 200 V for 30 min. The gel was soaked in 36 mM phosphate buffer (pH 7.8) containing 2 mM nitroblue tetrazolium for 30 min, rinsed with distilled water, and then transferred to 36 mM phosphate buffer (pH 7.8) containing 0.028 mM riboflavin and 28 mM TEMED (*N*,*N*,*N*′,*N*′-tetramethyl-ethylenediamine) for another 30 min. After being washed with distilled water, the gel was illuminated until white bands appeared. The SOD activity was verified by KCN and H_2O_2 as described by Kurepa et al. [27].

2.5. Detection and measurement of ROS in leaves

In situ detection of $O_2^{\bullet-}$ was performed by using the nitroblue tetrazolium (NBT) staining method as described by Kawai-Yamada et al. [28]. Detached leaves were vacuum-infiltrated with 10 mM NaN_3 in 10 mM potassium phosphate buffer (pH 7.8) for 1 min, and incubated in 1 mg ml^{-1} nitroblue tetrazolium (in 10 mM potassium phosphate buffer, pH 7.8) for 20 min in the dark at room temperature. In situ detection of H_2O_2 was performed by using the 3,3′-diaminobenzidine (DAB) staining method as described by Thordal-Christensen et al. [29]. Detached leaves were vacuum-infiltrated with 1 mg ml^{-1} DAB solution (pH 3.8) for 1 min and incubated in the dark at room temperature for 6 h. Stained leaves were cleared by boiling in acetic acid/glycerol/ethanol (1:1:3 [v/v/v]) solution before photographs were taken.

Total leaf H_2O_2 content was determined according to the method of Veljovic-Jovanovic et al. [30] as described previously [26].

2.6. Enzyme measurements

Total superoxide dismutase (SOD, EC1.15.1.1) activity was estimated by its ability to inhibit photoreduction of nitroblue tetrazolium as described previously [26]. Activities of the different SOD isoforms were determined by using 3 mM KCN or 5 mM H_2O_2 as the final concentration in the reaction mixture. KCN inhibits Cu/ZnSOD and H_2O_2 inhibits both FeSOD and Cu/ZnSOD activities. In order to determine the chloroplastic Cu/ZnSOD activity, the intact chloroplast was isolated [26].

Peroxidase activity (POX, EC1.11.1.7) was analyzed according to Ros-Barceló [31]. The activities of ascorbate peroxidase (APX, EC1.11.1.11) and catalase (CAT, EC1.11.1.6) were determined as described previously [26]. Glutathione peroxidase activity (GPX, EC1.11.1.9) was assayed spectrophotometrically as described by Yoshimura et al. [32].

2.7. Chlorophyll (Chl) fluorescence analysis

Chl fluorescence was measured using a PAM-2000 portable chlorophyll fluorometer (Heinz Walz, Germany). After a dark adaptation period of 30 min, minimum fluorescence (Fo) was determined by a weak red light. Maximum fluorescence of dark-adapted state (Fm) was measured during a subsequent saturating pulse of white light

(8000 μmol m^{-2} s^{-1} for 0.8 s). The leaf was then continuously illuminated with actinic light at an intensity of 100 μmol m^{-2} s^{-1} (which is equivalent of growth light intensity) for about 5 min. The steady-state fluorescence (Fs) was thereafter recorded and a second saturating pulse of white light (8000 μmol m^{-2} s^{-1} for 0.8 s) was imposed to determine the maximum fluorescence level in the light-adapted state (Fm′). The actinic light was removed and the minimal fluorescence level in the light-adapted state (Fo′) was determined by illuminating the leaf with a 3-s pulse of far-red light. Using above fluorescence parameters, we calculated: (1) the maximal efficiency of PSII photochemistry in the dark-adapted state, Fv/Fm = (Fm − Fo)/Fm; (2) the actual PSII efficiency, ΦPSII = (Fm′ − Fs)/Fm′; and (3) the photochemical quenching coefficient, qP = (Fm′ − Fs)/(Fm′ − Fo′).

The light-induced P700 absorbance changes at 820 nm were measured using the PAM-101 fluorometer connected to an emitter–detector unit ED 800 T (Walz) as described by Meurer et al. [33]. Absorbance changes induced by saturating far-red light were used to estimate the photochemical capacity of PSI.

2.8. Chl fluorescence relaxation kinetics

The decay of Chl *a* fluorescence yield after a single turnover flash was measured with a double-modulation fluorescence fluorometer (model FL-200, Photon Systems Instruments, Brno, Czech Republic). The instrument contained red LEDs for both actinic (20 μs) and measuring (2.5 μs) flashes, and was used in the time range of 100 μs–100 s. Before measurements, the tobacco leaves were dark adapted for 30 min in the presence or absence of 50 μM DCMU. The intensity of the measuring flashes was set at a value that was low enough to avoid reduction of Q_A in the presence of DCMU.

2.9. Thermoluminescence (TL) measurements

TL measurements of leaves were performed with the thermoluminescence extension of the Double-Modulated Fluorometer FL2000-S/F, consisting of Thermoregulator TR2000 (Photon Systems Instruments, Brno, Czech Republic). After a 30-min dark adaptation at 20 °C, the samples were cooled to −5 °C and excited with one or multiple number of single-turnover flashes. Then the samples were warmed up to 60 °C at a heating rate of 1 °C·s^{-1} and the TL light emission was measured during the heating. For $S_2Q_A^-$ recombination studies, leaves were measured in the presence of 50 μM DCMU before the flash illumination. Decomposition analysis of the TL glow curves was performed by a non-linear, least squares algorithm that minimizes the χ^2 function using a Microcal™ Origin™ Version 6.0 software package (Microcal Software Inc., Northampton, MA).

2.10. Measurements of electron transport activity

Thylakoid membranes were isolated as described by Peng et al. [34]. PSI electron transport activity was measured at saturating white light using a Clark-type oxygen electrode (Hansatech, King's Lynn, Norfolk, UK) and a 1-ml reaction mixture composed of 50 mM Tricine–NaOH (pH 7.5), 400 mM sucrose, 10 mM NaCl, 5 mM $MgCl_2$, 1 mM sodium azide, 0.5 mM methyl viologen, 10 μM DCMU, 1 mM sodium ascorbate, 200 μM 2,6-dichlorophenol indophenol (DCPIP), and thylakoids corresponding to 10 μg of chlorophyll. PSII electron transport activity was assayed in a 1-ml reaction mixture composed of 50 mM Mes–NaOH (pH 6.5), 400 mM sucrose, 50 mM $CaCl_2$, 5 mM $MgCl_2$, 0.2 mM 2,6-dichloro-*p*-benzoquinone (DCBQ), 1 mM ferricya, and thylakoids corresponding to 30 μg of chlorophyll.

2.11. Photoinhibition and recovery treatments

Detached leaves from transgenic and wild type plants grown under low light conditions (20 μmol m^{-2} s^{-1}), floating adaxial side up on water, were irradiated with a high light (500 μmol m^{-2} s^{-1}). To examine the role of chloroplast-encoded protein synthesis in the susceptibility of leaves to photoinhibition, detached leaves were incubated with their petioles submersed in 1 mM lincomycin solution at an irradiance of 20 μmol m^{-2} s^{-1} for 3 h prior to photoinhibitory light treatment. The temperature was maintained at 25 °C during photoinhibition and recovery treatments.

2.12. BN-PAGE, SDS-PAGE, and immunoblot analysis

BN-PAGE was performed using acrylamide gels with linear 6% to 12% gradients basically according to Peng et al. [34]. For immunoblot analysis, either total leaf proteins or thylakoid membrane proteins were separated using 15% SDS polyacrylamide gels containing 6 M urea [35]. After electrophoresis, the proteins were transferred to nitrocellulose membranes (Amersham Biosciences, USA), probed with specific primary antibodies, and visualized by the enhanced chemiluminescence method. X-ray films were scanned and analyzed using ImageMaster™ 2D Platinum software.

2.13. Measurements of chlorophyll and protein

Chl content was determined according to Arnon [36]. Protein content was determined by the dye-binding assay according to Bradford [37].

3. Results

3.1. Generation of transgenic tobacco plants exhibiting decreased FeSOD

To investigate the function of FeSOD in chloroplasts, we adopted RNA interference approach (RNAi) to generate transgenic tobacco plants with decreased FeSOD. Three independent RNAi lines (i4, i29, i34) which showed strong and stable gene silencing were chosen to obtain progeny (T_2 generation) and used for subsequent analyses. FeSOD mRNA level was significantly suppressed in the three RNAi lines as compared to that in wild type (WT) plants (Fig. 1A). Quantitative analysis using real-time PCR also showed that the amount of FeSOD transcript in transgenic i4, i29 and i34 RNAi lines was decreased to about 8% of that in WT plants (Fig. 1B). Immunoblotting analysis showed that there was a significant decrease in FeSOD protein as it was undetectable in the three RNAi lines (Fig. 1C). SOD activity gels analyses demonstrated that FeSOD activity was not detectable in the three RNAi lines (Fig. 1D).

3.2. Phenotypes of transgenic tobacco plants

Compared with WT plants, the three RNAi lines showed pale-green leaves when grown under normal light conditions (100 μmol m^{-2} s^{-1}), and the young leaves of transgenic tobacco plants showed more pronounced phenotypes than old mature leaves. Transgenic plants showed a significant decrease in Chl content and Fv/Fm values (Fig. 2). However, the phenotypic differences between transgenic and WT plants were alleviated significantly when grown under low light conditions (20 μmol m^{-2} s^{-1}). The pale green phenotype was almost invisible and there was only a small decrease in Chl content and Fv/Fm values when transgenic plants grown under low light (Fig. 2).

3.3. ROS accumulation in transgenic and wild type plants

Since transgenic tobacco plants exhibited pale-green phenotypes under normal light conditions and such a phenotype was almost invisible under low light intensity, we assumed that transgenic plants are very likely to suffer from photooxidative stress under normal light conditions which may be possibly due to substantial accumulation of ROS. To assess the possibility, NBT and DAB staining were performed in transgenic and WT plants to detect $O_2^{\bullet-}$ and H_2O_2, respectively.

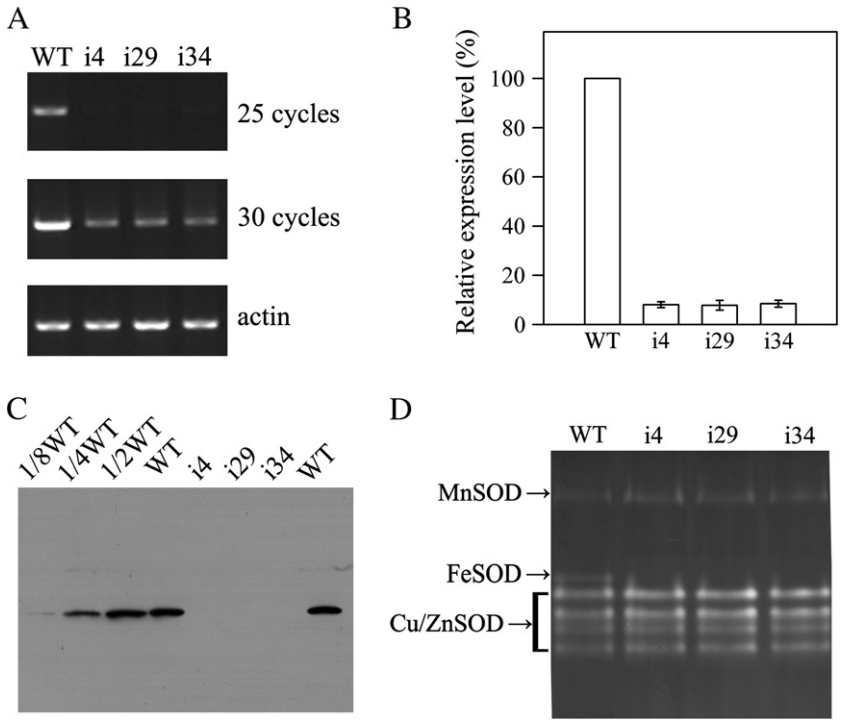

Fig. 1. (A) RT-PCR analyses in wild type (WT) and transgenic i4, i29, and i34 tobacco plants grown under normal light (100 μmol m^{-2} s^{-1}). RT-PCR was performed with specific primers for tobacco FeSOD and actin-specific primers. (B) Relative quantities of FeSOD transcripts by real-time RT-PCR analysis in wild type (WT) and transgenic i4, i29, and i34 tobacco plants grown under normal light (100 μmol m^{-2} s^{-1}). The transcript in wild type is given a value as 100%, and values are means ± SD of three replicates. (C) Immunoblot analysis of FeSOD protein in wild type (WT) and transgenic i4, i29, and i34 tobacco plants grown under normal light (100 μmol m^{-2} s^{-1}). (D) SOD activity gel analysis of wild type (WT) and transgenic i4, i29, and i34 tobacco plants grown under normal light (100 μmol m^{-2} s^{-1}).

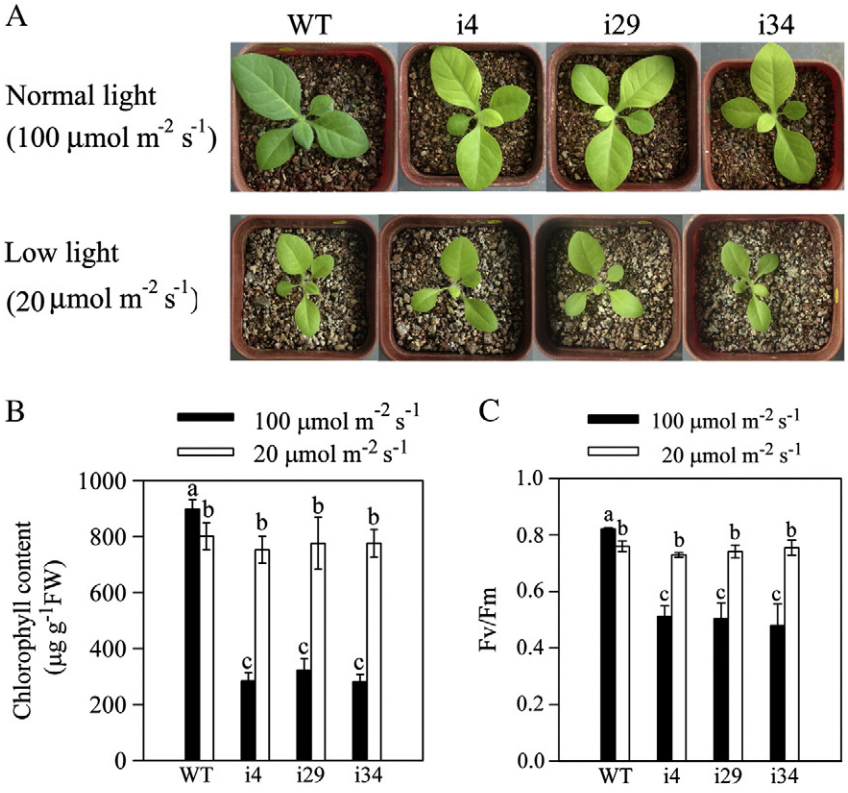

Fig. 2. (A) Phenotypes of wild type (WT) and transgenic i4, i29, and i34 tobacco plants grown under normal light (100 μmol m^{-2} s^{-1}) and low light conditions (20 μmol m^{-2} s^{-1}). (B) Total chlorophyll content in wild type (WT) and transgenic i4, i29, and i34 plants grown under normal light (100 μmol m^{-2} s^{-1}) and low light conditions (20 μmol m^{-2} s^{-1}). (C) The maximum efficiency of photosystem II photochemistry (Fv/Fm) in wild type (WT) and transgenic i4, i29, and i34 tobacco plants grown under normal light (100 μmol m^{-2} s^{-1}) and low light conditions (20 μmol m^{-2} s^{-1}). Values are means ± SD of four independent experiments. Different letters indicate significant difference between the different lines (ANOVA $posthoc_{LSD}$, $P<0.05$).

Under normal light conditions, NBT staining shows that there was a substantial accumulation of $O_2^{\bullet-}$ in transgenic plants as compared to that in WT plants (Fig. 3A). However, DAB staining suggests that H_2O_2 accumulated at very low levels and no obvious differences were observed between transgenic and WT plants (Fig. 3B). Though DAB staining is the most frequently used method for H_2O_2 detection in leaves, it has been demonstrated recently that DAB applied at the concentration of 1–2 mg ml^{-1} may result in a decrease in the efficiency of PSII photochemistry [38]. Thus, when NBT and DAB are infiltrated into the leaves, the toxicity of these probes cannot be neglected. We therefore tested the toxicity of NBT and DAB as used in this study on PSII photochemistry. The results in Table 1 show that NBT had no significant effect on Fv/Fm and ΦPSII, when the applied concentration (1 mg ml^{-1}) of NBT was infiltrated into the leaves of transgenic and WT plants and incubated for 20 min in the dark. However, with the applied concentration (1 mg ml^{-1}) and incubation time (6 h), DAB caused a significant decrease in Fv/Fm and ΦPSII. Since detection of H_2O_2 in vivo by DAB is affected by the activity of the intrinsic peroxidase [38], we also examined the changes in the activity of intrinsic peroxidase in transgenic and WT plants (Table 2). There were no significant differences in the activities of POX, GPX, and CAT between transgenic and WT plants. However, there was an increase in the activity of APX in transgenic plants. These results suggest that the NBT probe is suitable for the detection of $O_2^{\bullet-}$ and that the DAB probe is not suitable for the detection of H_2O_2 produced in the chloroplasts due to its toxicity on PSII photochemistry. Therefore, to determine in vivo H_2O_2 levels more accurately, we quantified leaf H_2O_2 using an improved spectrophotometric assay [30]. The quantitative measurements showed that there were no significant differences in the H_2O_2 content between transgenic and WT plants (Fig. 3C). We also investigated the contents of $HO^{\bullet}$ in transgenic and WT plants. We observed that there were no significant differences in the contents of $HO^{\bullet}$ between transgenic and WT plants (data not shown).

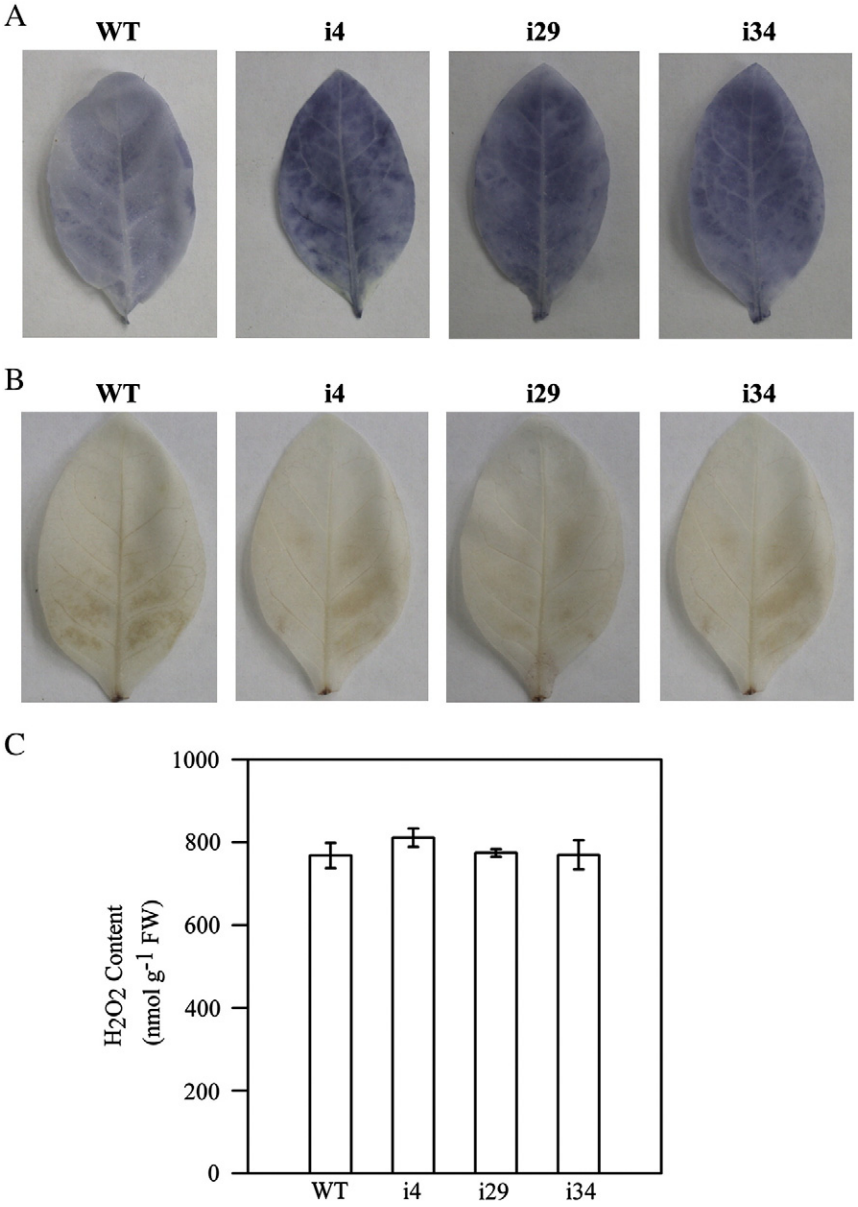

Fig. 3. (A) NBT staining for $O_2^{\bullet-}$ in leaves of wild type (WT) and transgenic i4, i29, and i34 tobacco plants grown under normal light (100 μmol m^{-2} s^{-1}). (B) DAB staining for H_2O_2 in leaves of wild type (WT) and transgenic i4, i29, and i34 tobacco plants grown under normal light (100 μmol m^{-2} s^{-1}). (C) Levels of H_2O_2 in leaves from wild type (WT) and transgenic i4, i29, and i34 tobacco plants grown under normal light (100 μmol m^{-2} s^{-1}). Values are means ± SD of four independent experiments.

Table 1
Effects of nitroblue tetrazolium (NBT, 1 mg ml^{-1}) and 3,3′-diaminobenzidine (DAB, 1 mg ml^{-1}) on Fv/Fm and ΦPSII in wild type (WT) and transgenic i4 tobacco plants grown under normal light (100 μmol m^{-2} s^{-1}).

	Fv/Fm	ΦPSII
WT (Control, 20 min)	0.82 ± 0.03	0.60 ± 0.01
WT (NBT, 20 min)	0.80 ± 0.03	0.59 ± 0.03
i4 (Control, 20 min)	0.51 ± 0.04	0.35 ± 0.03
i4 (NBT, 20 min)	0.50 ± 0.03	0.34 ± 0.02
WT (Control, 6 h)	0.78 ± 0.02	0.56 ± 0.01
WT (DAB, 6 h)	0.65 ± 0.01	0.39 ± 0.02
i4 (Control, 6 h)	0.48 ± 0.02	0.33 ± 0.01
i4 (DAB, 6 h)	0.39 ± 0.01	0.23 ± 0.01

Control represents infiltration with phosphate buffer (as control for NBT) or water (as control for DAB). Similar results were obtained in transgenic i29 and i34 tobacco plants (data not shown). Means ± SD values were calculated from four independent experiments.

3.4. Activities of different forms of SOD in transgenic and wild type plants

In order to further investigate the effect of decreased FeSOD on the activities of different forms of SOD, we measured the activities of different forms of SOD using KCN or H_2O_2 inhibition. As shown in Table 3, there were significant increases in the activities of both MnSOD and Cu/ZnSOD in transgenic plants, which resulted in enhanced total SOD activities. We further investigated if there was an increase in the chloroplastic Cu/ZnSOD activity. The intact chloroplasts were isolated and then chloroplastic Cu/ZnSOD activities were determined in transgenic and WT plants. Our results show that the chloroplastic Cu/ZnSOD activity was also significantly increased in transgenic plants.

3.5. PSI and PSII activities in transgenic and wild type plants

Table 4 shows some parameters related to the functions of PSI and PSII in transgenic and WT plants. There was a significant decrease in Fv/Fm, ΦPSII, and PSII electron transport activity in transgenic plants as compared to that in WT plants. The values of Fv/Fm, ΦPSII, and PSII electron transport activity in transgenic plants were about 60%, 55%, and 50% of those of WT plants, respectively. qP was not strongly affected in transgenic tobacco plants compared with WT plants (Table 4), indicating that the electrons released by PSII could be transported through the electron transport chain and the subsequent photosynthetic electron chain (i.e. the cytochrome b6/f complex and PSI) was functional [39]. The functional state of the PSI can be assessed by measuring the absorbance changes around 820 nm [33]. There was about 20% decrease in an absorbance change of P700 in transgenic plants compared to that in WT plants. Also, there was a decrease in PSI electron transport activity in transgenic plants, which was about 83% of that of WT plants.

3.6. The properties of both the donor and acceptor side of PSII in transgenic and wild type plants

The above results demonstrate that PSII function was profoundly affected in transgenic plants. We thus further investigated how the acceptor and donor side functions of PSII were affected. To this purpose, the flash-induced increase and subsequent relaxation of fluorescence yield was performed from intact leaves of transgenic and WT plants in the absence and presence of DCMU.

In the absence of DCMU, the relaxation of the flashed induced increase in variable Chl fluorescence yield in transgenic and WT plants can be resolved into three exponential decay components (Fig. 4A, B, Table 5). The fast phase, which is related to the electron transfer from Q_A^- to Q_B in PSII reaction centers having an occupied Q_B pocket at the time of flashing, showed a significant increase in the decay half time but a decrease in the amplitude in transgenic plants compared with WT plants. The $t_{1/2}$ of the fast phase increased from 295 μs in WT plants to about 470 μs in transgenic plants. The amplitude of the fast phase decreased from 67% in WT plants to 57% in transgenic plants. The middle phase is associated with the electron transfer from Q_A^- to Q_B in PSII reaction centers that have an empty Q_B pocket at the time of flashing and have to bind plastoquinone to the Q_B site from the pool before Q_A^- reoxidation. For the middle phase, the decay half time was noticeably increased in transgenic plants and the amplitude was also slightly higher in transgenic plants compared with WT plants. The $t_{1/2}$ of the middle phase increased from 6.4 μs in WT plants to about 13.0 μs in transgenic plants. The amplitude of the middle phase also increased from 18% in WT plants to about 21% in transgenic plants. The slow phase, which is related to the reoxidation of Q_B^- with the S_2 state of the OEC via $Q_A^-Q_B \leftrightarrow Q_AQ_B^-$ equilibrium [40], demonstrated a significant decrease in the decay half time but an increase in the amplitude in transgenic plants compared with WT plants. The $t_{1/2}$ of the slow phase decreased from 6.8 s in WT plants to about 2.3 s in transgenic plants. The amplitude of the slow phase increased from 16% in WT plants to about 22% in transgenic plants.

In the presence of DCMU, which prevents the electron transfer from Q_A^- to Q_B, the fluorescence relaxation reflects the reoxidation of Q_A^- via recombination with the donor-side components. In the presence of DCMU, the fluorescence relaxation was dominated by a slow component in transgenic and WT plants, and the slow phase arose from the reoxidation of Q_A^- with the S_2 state of the OEC. As shown in Fig. 4C, D and Table 5, there were no significant differences in the fluorescence relaxation kinetics between transgenic and WT plants.

Table 2
Activities of intrinsic peroxidase in leaves of wild type (WT) and transgenic tobacco plants grown under normal light (100 μmol m^{-2} s^{-1}).

	POX activity	APX activity	GPX activity	CAT activity
WT	174.47 ± 9.68	0.97 ± 0.03	25.71 ± 1.15	90.08 ± 5.92
i4	178.49 ± 14.15	1.67 ± 0.04	26.93 ± 1.97	90.66 ± 7.63
i29	179.88 ± 17.20	1.73 ± 0.03	26.52 ± 2.61	90.27 ± 4.60
i34	175.13 ± 6.78	1.69 ± 0.03	26.02 ± 2.81	91.95 ± 6.68

Means ± SD values were calculated from three independent experiments. POX, APX, and CAT activities were expressed as μmol mg^{-1} protein min^{-1}. GPX activity was expressed as nmol mg^{-1} protein min^{-1}.

Table 3
SOD activities in wild type (WT) and transgenic tobacco plants grown under normal light (100 μmol m^{-2} s^{-1}).

SOD activity (units mg^{-1} protein)	WT	i4	i29	i34
Total SOD	10.79 ± 0.24	15.59 ± 0.55	16.04 ± 0.28	16.23 ± 0.26
MnSOD	0.87 ± 0.02	1.42 ± 0.05	1.49 ± 0.02	1.46 ± 0.02
FeSOD	1.27 ± 0.03	n.d.	n.d.	n.d.
Cu/ZnSOD	8.65 ± 0.19	14.16 ± 0.50	14.55 ± 0.26	14.77 ± 0.24
$_{chl}$Cu/ZnSOD	2.46 ± 0.05	5.21 ± 0.08	5.39 ± 0.08	5.41 ± 0.15

n.d. represent not detectable. Means ± SD values were calculated from four independent experiments.

Table 4
Spectroscopic data and electron transport activities in wild type (WT) and transgenic tobacco plants grown under normal light (100 μmol m^{-2} s^{-1}).

	WT	i4	i29	i34
Fv/Fm	0.82 ± 0.01	0.51 ± 0.04	0.50 ± 0.06	0.48 ± 0.08
ΦPSII	0.60 ± 0.01	0.35 ± 0.04	0.33 ± 0.02	0.34 ± 0.01
qP	0.81 ± 0.01	0.72 ± 0.02	0.69 ± 0.01	0.71 ± 0.04
ΔA_{820max} (%)	100	79 ± 2	78 ± 3	81 ± 2
PSII activity (μmol O_2 mg^{-1} Chl h^{-1})	140 ± 1	68 ± 1	72 ± 1	72 ± 2
PSI activity (μmol O_2 mg^{-1} Chl h^{-1})	643 ± 12	533 ± 4	532 ± 8	540 ± 9

Means ± SD values were calculated from three independent experiments.

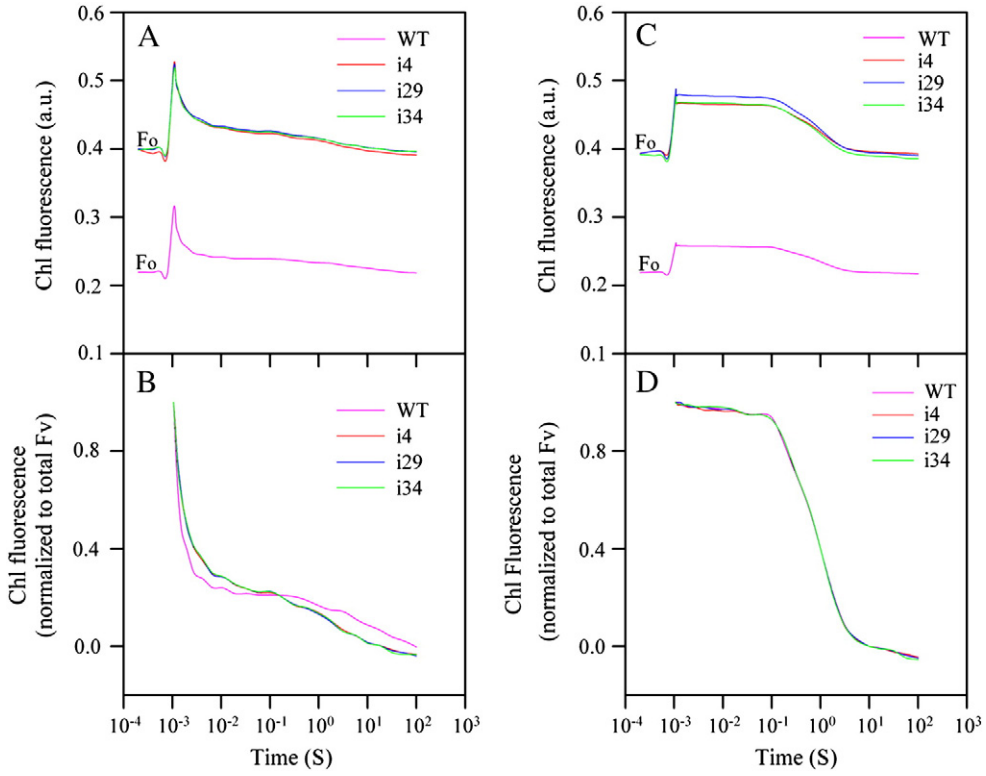

Fig. 4. Relaxation of flash-induced fluorescence yield in leaves of wild type (WT) and transgenic i4, i29, and i34 tobacco plants grown under normal light (100 μmol m^{-2} s^{-1}). (A) The curves were the actual data of the fluorescence signals in the absence of 50 μM DCMU. (B) The curves were normalized relative to the total variable fluorescence in the absence of 50 μM DCMU. (C) The curves were the actual data of the fluorescence signals in the presence of 50 μM DCMU. (D) The curves were normalized relative to the total variable fluorescence in the presence of 50 μM DCMU.

It should be noted that the Fo level in transgenic tobacco plants was about two times higher than in wild type (Fig. 4A, C). The increase in Fo may reflect more free LHCII accumulated in transgenic plants than in WT plants.

TL was further used to investigate the redox properties of the acceptor and donor sides of PSII in transgenic and WT plants.

Table 5
Parameters of decay kinetics of flash-induced variable fluorescence in wild type (WT) and transgenic tobacco plants grown under normal light (100 μmol m^{-2} s^{-1}).

	Total amplitude (%)	Fast phase	Middle phase	Slow phase
		$t_{1/2}$ (μs) [A (%)]	$t_{1/2}$ (ms) [A (%)]	$t_{1/2}$ (s) [A (%)]
Without DCMU				
WT	100[a]	295 ± 30	6.4 ± 0.4	6.8 ± 0.4
		(66.7 ± 3.1)[b]	(17.8 ± 0.6)	(15.5 ± 0.3)
i4	95 ± 2	464 ± 47	13.0 ± 0.7	2.5 ± 0.2
		(57.0 ± 2.6)	(20.2 ± 0.8)	(22.9 ± 0.2)
i29	94 ± 3	472 ± 52	12.2 ± 0.6	2.2 ± 0.3
		(56.9 ± 3.0)	(20.9 ± 0.8)	(22.2 ± 0.3)
i34	95 ± 2	465 ± 52	12.6 ± 0.5	2.3 ± 0.3
		(57.0 ± 3.3)	(20.9 ± 0.9)	(22.1 ± 0.3)
With DCMU				
WT	100	– (0)	– (0)	1.11 ± 0.04 (100)
i4	100	– (0)	– (0)	1.12 ± 0.04 (100)
i29	100	– (0)	– (0)	1.10 ± 0.04 (100)
i34	100	– (0)	– (0)	1.10 ± 0.03 (100)

The relaxation of the flashed-induced fluorescence yield was measured without or with 50 μM DCMU. Mean ± SD values were calculated from four to six independent experiments.

[a] Values represent the amplitude of total variable fluorescence as a percentage of that in wild type plants.

[b] Values in parentheses are relative amplitude as a percentage of total variable fluorescence obtained from wild type and transgenic tobacco plants.

Recombination of positive charges stored in the S_2 and S_3 oxidation states of the water-oxidizing complex with electrons stabilized on the reduced Q_A and Q_B acceptors of PSII results in characteristic TL emissions [41,42]. The TL intensity reflects the amount of recombining charges, whereas the peak temperature is indicative of the energetic stabilization of the separated charge pair; the higher the peak temperature, the greater the stabilization [43]. Illumination of single turnover flash with the plant sample after a short dark adaptation induces a major TL band, called the B-band which appears around at 30 °C and arises from $S_2/S_3Q_B^-$ recombination [42,44,45]. If electron transfer between Q_A and Q_B is blocked by DCMU, the B-band is replaced by the so-called Q-band arising from $S_2Q_A^-$ recombination at around 10 °C [44].

As shown in Fig. 5A and Table 6, the peak temperature for the $S_2Q_B^-$ charge recombination was downshifted from 35.7 °C in WT plants to about 32 °C in transgenic plants, indicating that the stabilization of the $S_2Q_B^-$ charge pair was decreased in transgenic plants. Since the contribution of the B-band compared to other TL bands is complex, we further performed decomposition analysis of the TL glow curves. The best fit of the curve yielded three distinct peaks with characteristic temperatures corresponding to the B_1, B_2 and AG luminescence, respectively and no Q-band was decomposed (Table 7). The afterglow (AG) band is a B-type recombination that depends on the back transfer of electrons from stroma to the acceptor side of PSII [46]. Our results show that the peak temperatures of B1, B2, and AG bands were downshifted and their areas decreased significantly in transgenic plants (Table 7).

In the presence of DCMU, the peak temperature for the $S_2Q_A^-$ charge recombination in transgenic plants was comparable with that in WT plants (Fig. 5B, Table 6). Moreover, since the $S_2Q_B^-$ recombination was destabilized but the $S_2Q_A^-$ recombination was unaffected in transgenic tobacco plants, it seems that the change in TL emission maxima for the

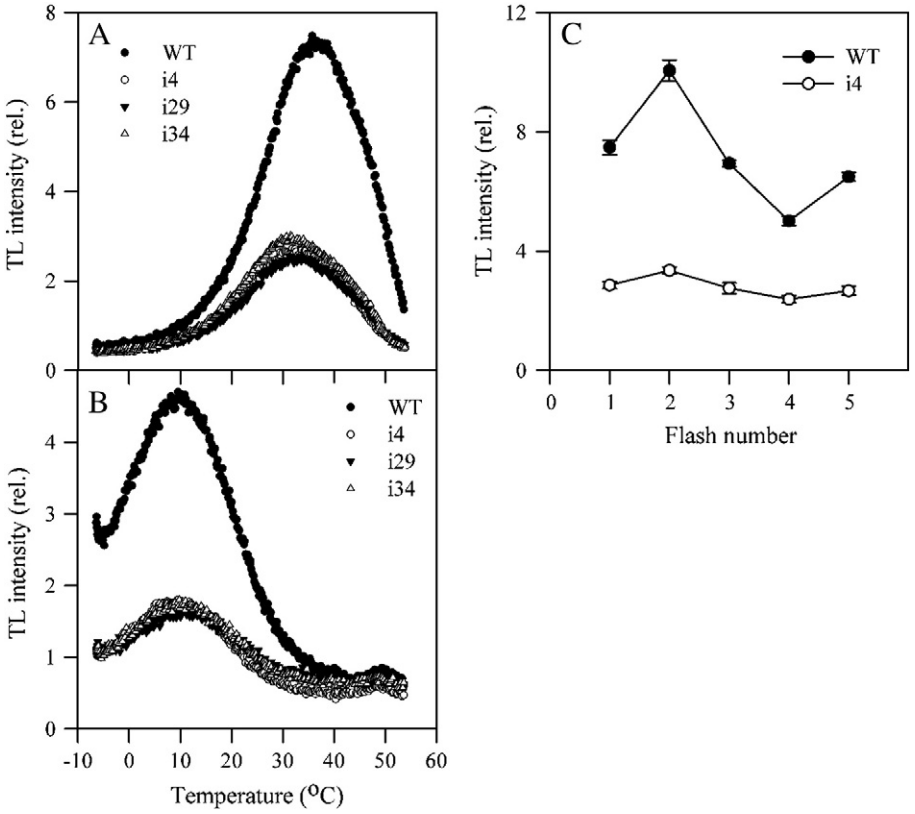

Fig. 5. (A) Thermoluminescence glow curves in wild type (WT) and transgenic i4, i29, and i34 tobacco plants grown under normal light (100 μmol m^{-2} s^{-1}). The leaves were excited with a single flash in the absence of 50 μM DCMU. (B) Thermoluminescence glow curves in wild type (WT) and transgenic i4, i29, and i34 tobacco plants grown under normal light (100 μmol m^{-2} s^{-1}). The leaves were excited with a single flash in the presence of 50 μM DCMU. (C) The flash-induced oscillation of the B thermoluminescence band in wild type (WT) and transgenic i4 plants grown under normal light (100 μmol m^{-2} s^{-1}). Values are means ± SD of four independent experiments.

$S_2Q_B^-$ in transgenic plants was due to a modification of in the redox properties of Q_B and the redox properties of the S_2 state were not affected in transgenic plants.

Fig. 5C shows the oscillation of the intensity of the B-band in WT and transgenic i4 plants. WT leaves showed typical oscillation with a periodicity of four with the maximum emission occurring on the second flash. However, the oscillation pattern in transgenic i4 plants was damped as compared to that in WT plants. Similar results were also observed in transgenic i29 and i34 plants (data not shown).

3.7. Contents of PSII proteins in transgenic and wild type plants

We further investigated the contents of PSII proteins (D1, CP47, CP43, LHCII, and PsbO) and other photosynthetic membrane protein contents (PsaA/B for PSI, Cytf for cytochrome b6f, and CF1β for ATP synthase) in transgenic and WT plants (Fig. 6A). Our results showed that levels of the plastid-encoded PSII core subunits D1, CP47 and CP43 in transgenic plants were reduced to approximately 65% of those of WT plants. However, the levels of nucleus-encoded PSII proteins, extrinsic protein PsbO of the oxygen-evolving complex, and antenna protein LHCII in transgenic plants were comparable with those of WT plants. The content of PsaA/B in transgenic plants was reduced to 85% of that of WT plants, while the contents of Cytf and CF1β in transgenic plants were similar to those of WT plants.

We further analyzed thylakoid membrane complexes of transgenic and WT plants by BN-PAGE and subsequent SDS-PAGE (Fig. 6B, C). In the first dimension, the native thylakoid membrane complexes were separated into six major bands which represent PSII supercomplexes (band I), monomeric PSI and dimeric PSII (band II), monomeric PSII (band III), CP43-free PSII (band IV), trimeric LHCII (band V), and monomeric LHCII (band VI) [47]. The first-dimensional BN-PAGE analysis showed that the amounts of chlorophyll-containing protein complexes (labeled I and II) and monomeric PSII (labeled III) were significantly reduced in transgenic plants when equal amounts of chlorophyll were loaded (Fig. 6B). Analyses of the SDS-PAGE gels followed by the BN-PAGE confirmed that the amounts of the PSII core subunits D1, D2, CP47, and CP43 were markedly reduced in transgenic plants, especially the PSII supercomplexes and PSII dimer, which contained only trace amounts of PSII core proteins (Fig. 6C). In addition, the amounts of PSI subunits were also reduced in transgenic plants, but the reduction was not as obvious as in the PSII core

Table 6
Peak emission temperatures of the TL curves in wild type (WT) and transgenic tobacco plants grown under normal light (100 μmol m^{-2} s^{-1}).

	Peak temperature (°C)	
	Without DCMU	With DCMU
WT	35.7 ± 0.4	9.5 ± 0.1
i4	32.1 ± 0.3	9.7 ± 0.3
i29	31.8 ± 0.3	9.8 ± 0.3
i34	31.9 ± 0.3	9.7 ± 0.1

The measurements were performed in the absence and presence of 50 μM DCMU. Mean ± SD values were calculated from four to six independent experiments.

Table 7
Peak emission temperatures (°C) and relative peak area (A) of the Gaussian sub-bands for thermoluminescence B-band in wild type (WT) and transgenic tobacco plants grown under normal light (100 μmol m^{-2} s^{-1}).

	B1 (°C) [A_1]	B2 (°C) [A_2]	AG (°C) [A_3]
WT	26.9 ± 0.5 (1.63 ± 0.06)	37.0 ± 0.2 (6.01 ± 0.32)	46.5 ± 0.6 (1.23 ± 0.15)
i4	22.5 ± 0.1 (0.65 ± 0.05)	32.6 ± 0.7 (2.11 ± 0.21)	44.8 ± 0.1 (0.69 ± 0.01)
i29	23.1 ± 0.7 (0.65 ± 0.02)	33.5 ± 0.7 (2.03 ± 0.06)	44.6 ± 0.7 (0.68 ± 0.01)
i34	22.7 ± 0.7 (0.63 ± 0.03)	32.9 ± 0.5 (2.01 ± 0.13)	44.8 ± 0.4 (0.62 ± 0.03)

Mean ± SD values were calculated from four to six independent experiments.

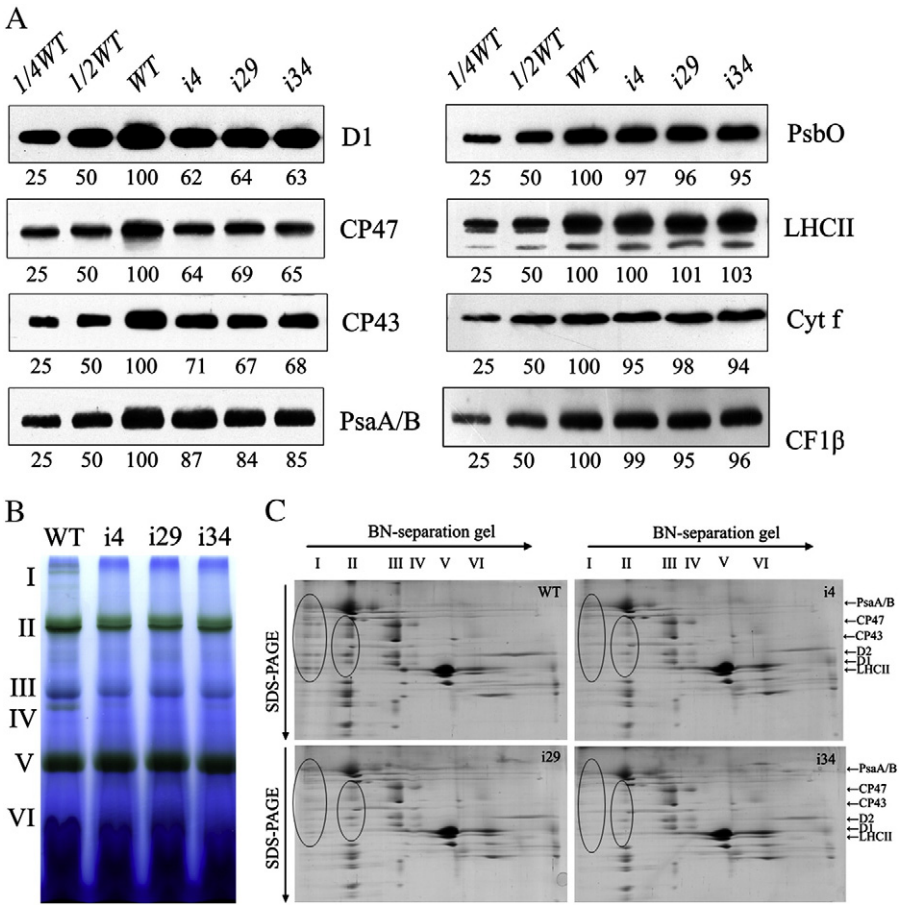

Fig. 6. (A) Immunodetection of thylakoid membrane proteins (1 μg chlorophyll) in wild type (WT) and transgenic i4, i29, and i34 tobacco plants grown under normal light (100 μmol m^{-2} s^{-1}). The percentage protein levels shown below the lanes were estimated by comparison with levels of corresponding thylakoid proteins of WT. (B) BN gel analysis of thylakoid membrane protein complexes (10 μg chlorophyll) in wild type (WT) and transgenic i4, i29, and i34 tobacco plants grown under normal light (100 μmol m^{-2} s^{-1}). (C) Two-dimensional separation of protein complexes in the thylakoid membranes in wild type (WT) and transgenic i4, i29, and i34 tobacco plants.

subunits (Fig. 6C). It should be noted that the results in Fig. 6 were obtained on the basis of equal chlorophyll but very similar results were also observed when analyzed on the basis of equal protein.

3.8. Photoinhibition in transgenic and wild type plants

The above results show that the Fv/Fm values were significantly decreased in transgenic plants compared with WT plants when grown under normal light conditions (100 μmol m^{-2} s^{-1}) whereas transgenic plants showed only a slight decrease in Fv/Fm when grown under low light conditions (20 μmol m^{-2} s^{-1}) (Fig. 2C), suggesting that transgenic plants were already subjected to photooxidative stress even under normal light conditions. To further investigate the function of FeSOD in protecting photosynthesis against photooxidative stress, we examined the sensitivity of photoinhibition in transgenic and WT plants when subjected to high light treatment (500 μmol m^{-2} s^{-1}). Since the pale-green phenotype in transgenic plants was almost not visible and transgenic plants showed only a slight decrease in Fv/Fm as compared with that in WT plants when grown under low light conditions, transgenic and WT plants grown under low light conditions were chosen and exposed to high light treatment. Fig. 7A shows the changes in Fv/Fm in transgenic and WT plants during high light treatment. In the absence of lincomycin, there was a significant decrease in Fv/Fm in transgenic and WT plants during high light treatment. However, such a decrease was much greater in transgenic plants than in WT plants. In the presence of lincomycin, the decrease in Fv/Fm was more rapid and the decrease in Fv/Fm in transgenic plants was still greater than in WT plants (Fig. 7A). For example, after 4-h high light treatment, Fv/Fm was about 0.1 in WT plants but reached zero in transgenic plants due to loss of variable fluorescence. Since lincomycin blocks PSII repair process by inhibiting de novo protein synthesis in the chloroplast, the decrease in Fv/Fm reflects the rate of PSII photodamage. Thus, the above results demonstrate that transgenic plants had accelerated rate of photodamage compared with WT plants.

To further investigate whether the PSII repair process of transgenic plants was affected, the recovery of Fv/Fm in transgenic and WT plants after high light treatments was monitored. In this experiment, high light treatment resulted in about a 50% decrease in Fv/Fm in both transgenic and WT plants. We observed that the recovery of Fv/Fm after photoinhibition in transgenic plants was very similar to that in WT plants (Fig. 7B). Therefore, the increased susceptibility of transgenic plants to photoinhibition was due mainly to accelerated PSII photodamage rather than inhibited PSII repair process.

To further examine whether increased susceptibility of transgenic plants to photoinhibition is related to the stability of PSII proteins, we investigated the changes in the contents of PSII proteins in transgenic and WT plants during high light treatment (Fig. 8). In the absence of lincomycin, the content of D1 protein declined rapidly in both transgenic and WT plants during high light treatment and such a decline was greater in transgenic plants than in WT plants. Compared to the content of D1 protein, the contents of D2, CP47 and CP43 proteins were relatively stable, although the contents of these proteins also showed a decrease finally and this decrease was greater in transgenic plants than in WT plants (Fig. 8A). These results are consistent with the notion that D1 protein exhibits the highest turnover rate of all thylakoid proteins [48]. In the presence of lincomycin, there was a significant

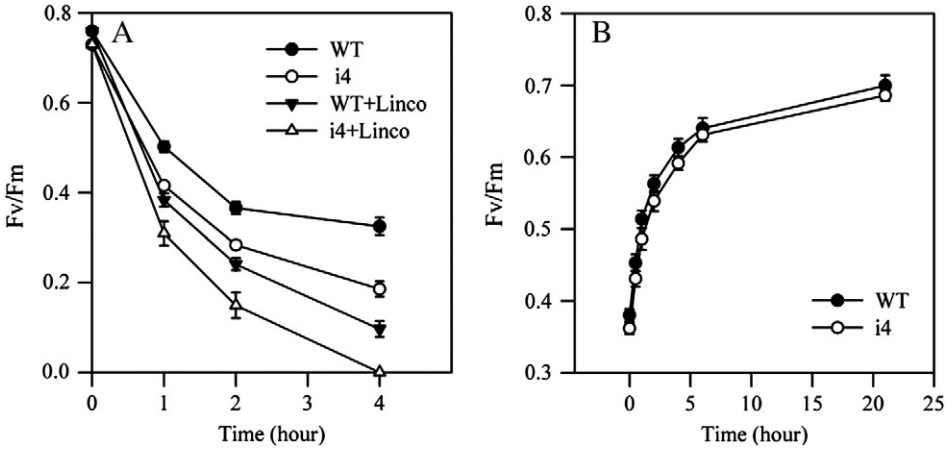

Fig. 7. (A) Photoinactivation of PSII activity under high-light illumination. The maximal photochemical efficiency of PSII (Fv/Fm) was measured for detached leaves from wild type (WT) and transgenic i4 plants grown under low light conditions (20 μmol m^{-2} s^{-1}) during exposure to irradiance of 500 μmol m^{-2} s^{-1} in the absence of lincomycin and in the presence of lincomycin. Similar results were obtained with the transgenic i29 and i34 tobacco plants (data not shown). Values are means ± SD of four independent experiments. (B) Recovery of maximum photochemical efficiency of PSII (Fv/Fm) after photoinhibition. Leaves of wild type (WT) and the transgenic i4 plants grown under low light conditions (20 μmol m^{-2} s^{-1}) were illuminated to induce 50% photoinhibition of PSII activity, and the recovery of Fv/Fm was subsequently followed at an irradiance of 20 μmol m^{-2} s^{-1}. Similar results were obtained with the transgenic i29 and i34 tobacco plants (data not shown). Values are means ± SD of four independent experiments.

decrease in the contents of D1, D2, CP47 and CP43 after being treated with high light for 4 h in transgenic and WT plants. However, D1 protein showed the greatest decrease among these proteins. Again, the decrease in the contents of D1, D2, CP47 and CP43 was greater in transgenic plants than in WT plants (Fig. 8B). We also examined the contents of subunits of other photosynthetic membrane complexes during high light treatment. There were no significant decreases in the levels of PsaA/B, cytf, and CF1β in both transgenic and WT plants during high light treatment (data not shown), indicating that the complexes of PSI, cytochrome b6f, and ATP synthase were stable during high light treatment.

We further examined the changes in the accumulation of $O_2^{\bullet-}$ in both transgenic and WT plants during high light treatment (Fig. 9). The accumulation of $O_2^{\bullet-}$ in both transgenic and WT plants was found to be increased with high light treatment and the level of $O_2^{\bullet-}$ was higher in transgenic plants than that in WT plants. We also examined the changes in the accumulation of $HO^{\bullet}$ and H_2O_2 in both transgenic and WT plants during high light treatment. We observed that although there were significant increases in the levels of $HO^{\bullet}$ and H_2O_2 during high light treatment in transgenic and WT plants, there were no significant differences in the levels of $HO^{\bullet}$ and H_2O_2 between transgenic and WT plants (data not shown).

4. Discussion

Chloroplastic FeSODs play important roles in protecting chloroplasts from photooxidative damage. However, the protecting mechanism is not fully understood. In this study, we obtained the transgenic tobacco plants with severely decreased chloroplastic FeSOD by RNAi. The effects of knockdown of the FeSOD protein on the PSII function and the possible mechanisms of FeSOD in protecting PSII against photooxidative stress are characterized.

It has been reported that damage occurs primarily at PSI in a cyanobacterium lacking detectable FeSOD activity [49]. However, our results demonstrate that PSII was severely impaired in transgenic tobacco plants, whereas the PSI was less affected (Table 4). Immunoblot and BN-PAGE analysis further corroborate these results. The amounts of the PSII core subunits were significantly reduced in transgenic tobacco plants, whereas the reduction in the content of PSI reaction center PsaA/B protein was much less and components of the cytochrome b6f complex and ATP synthase accumulated to the same levels as to WT plants (Fig. 6A, C). Taken together, these data suggest

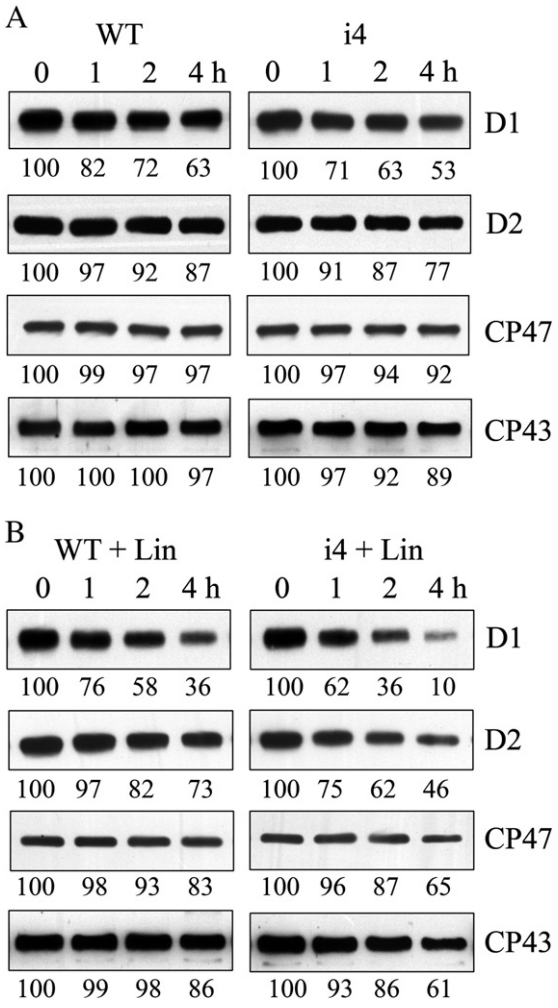

Fig. 8. Stability of PSII proteins. Leaves of wild type (WT) and transgenic i4 tobacco plants grown under low light conditions (20 μmol m^{-2} s^{-1}) were exposed to high-light illumination in the absence (A) or in the presence (B) of lincomycin for 1, 2, or 4 h. After this treatment, the thylakoid membranes were isolated and the contents of PSII proteins were determined through immunoblot analysis. Similar results were obtained with the transgenic i29 and i34 tobacco plants (data not shown). Percentage protein levels shown below the lanes were estimated by comparison with levels found in corresponding samples taken at time 0.

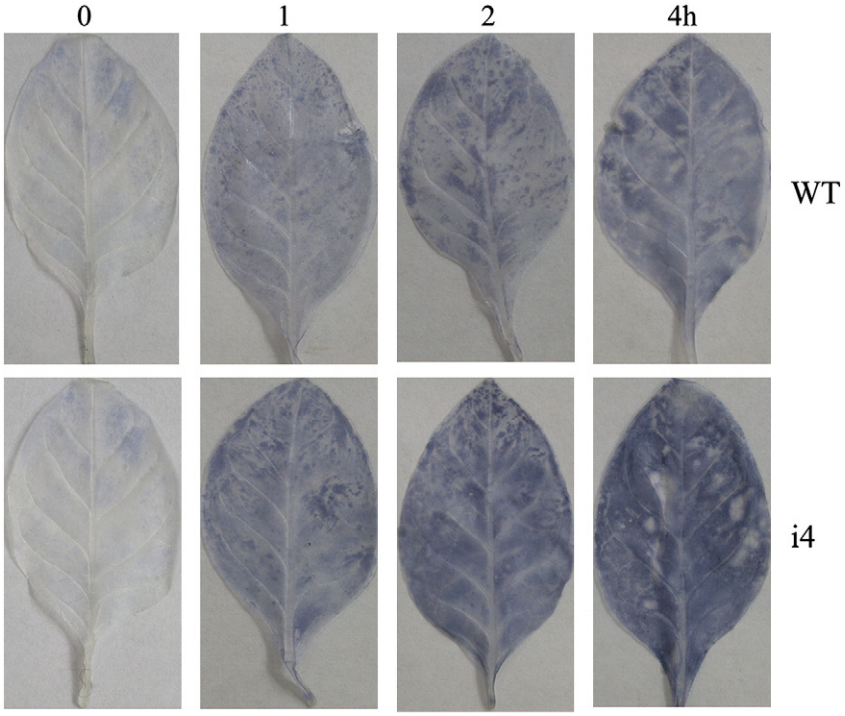

Fig. 9. $O_2^{\bullet-}$ accumulation in leaves of wild type (WT) and transgenic i4 tobacco plants under high-light illumination. Leaves of wild type (WT) and transgenic i4 tobacco plants grown under low light conditions (20 μmol m^{-2} s^{-1}) were exposed to high-light illumination for 1, 2, or 4 h. After this treatment, NBT staining was performed to detect the $O_2^{\bullet-}$ accumulation. Similar results were obtained with the transgenic i29 and i34 tobacco plants (data not shown).

that PSII in transgenic plants is primarily affected. We further investigated how PSII function is affected in transgenic plants.

In this study, we observed that in the presence of DCMU, the overall fluorescence relaxation kinetics in transgenic plants was comparable with that in WT plants (Fig. 4C, D, Table 5), indicating that decreased FeSOD has no effect on the donor side of PSII. Analyses of fluorescence decay kinetics showed a significant increase in the decay half time of the fast phase but a decrease in its amplitude in transgenic plants compared with WT plants (Fig. 4A, B, Table 5), suggesting that decreased FeSOD results in an inhibition of electron transfer from Q_A^- to Q_B (Q_B^-). Such an inhibition may be associated with a decrease in the apparent equilibrium constant for sharing the electron between Q_A and Q_B since we observed a decrease in the $t_{1/2}$ of the slow phase in the absence of DCMU ($t_{1/2}(S_2Q_AQ_B^-)$ but no changes in the $t_{1/2}$ of the slow phase in the presence of DCMU ($t_{1/2}(S_2Q_A^-)$ (Fig. 4, Table 5). The decreased apparent equilibrium might be associated with a decreased affinity of Q_B binding pocket as we observed an increased decay half time of the middle phase (Fig. 4A, B, Table 5). In addition, we observed a decrease in the stability of the $S_2Q_B^-$ charge recombination in transgenic plants, whereas the stability of the $S_2Q_A^-$ was not affected (Fig. 5, Table 6). These results indicate that the redox potential of Q_B is decreased in transgenic plants, while the redox potential of the S_2 state in transgenic plants is similar to that in WT plants.

An inhibition of electron transfer at the acceptor side of PSII in transgenic plants may result from modification of the Q_B niche. This modification could be due to conformational changes induced by $O_2^{\bullet-}$ attack. Although $O_2^{\bullet-}$ is thought to be mainly produced around PSI by Mehler reaction [50], it can propagate to the reaction center of PSII along or within the membrane [51]. Alternatively, $O_2^{\bullet-}$ may also be produced around PSII. It has been demonstrated that under limitation of electron transport reaction between PSI and PSII, $O_2^{\bullet-}$ can be generated on the PSII electron acceptor side, since the primary electron acceptor $Pheo^-$, Q_A^-, plastoquinol and cyt b_{559} are proposed to serve as the reductant of molecular oxygen [21,52,53]. It has been suggested that the plastoquinone binding site is accessible to lipophilic molecules [54]. In addition, we observed that there was accumulation of $O_2^{\bullet-}$ in transgenic plants (Fig. 3). Thus, a possible explanation for the modification of the Q_B niche in transgenic plants may be that the presence of the plastoquinone binding site allows access to $O_2^{\bullet-}$.

As discussed above, the modified acceptor side of PSII may be associated with modification of the potential of Q_B due to attack of $O_2^{\bullet-}$. However, there is a relatively large proportion of centers which have Q_B^- bound to the Q_B binding pocket in leaves even after long dark adaptation [55]. In addition, there may be a change in the reduction state of the plastoquinone pool due to the changes in reduction state of the chloroplast or metabolic changes in transgenic plants with low amount of FeSOD. Thus, the changes in the fluorescence decay kinetics and the TL curves may be also caused by a different reduction state of the plastoquinone pool and a higher degree of centers with Q_B^- present in the dark.

To address the question as to why the donor side of PSII is not affected, a reasonable explanation is that $O_2^{\bullet-}$ located at the Q_B niche cannot cross the membrane from the acceptor side to the donor side. However, it is well established that $O_2^{\bullet-}$ is in pH-dependent equilibrium with its protonated form hydroperoxyl radical ($HO_2^{\bullet}$). $HO_2^{\bullet}$ is able to diffuse through the membrane. $HO_2^{\bullet}$ dismutates spontaneously to free H_2O_2 at several orders of magnitude faster than $O_2^{\bullet-}$ does [21,53]. The long-lived H_2O_2 is an ideal candidate for this transportation [56]. However, there was no significant accumulation of H_2O_2 in transgenic plants (Fig. 3). Thus, our results seem to suggest that there was no significant accumulation of the protonated form of $O_2^{\bullet-}$, i.e. $HO_2^{\bullet}$, in transgenic plants.

Another characteristic feature of transgenic plants is the low accumulation of PSII proteins. Our BN-PAGE and subsequent SDS-PAGE analysis showed that levels of PSII dimers and PSII-LHCII supercomplexes were severely reduced in transgenic plants, whereas free LHCII monomers were increased (Fig. 6B, C). These results indicate that stability or assembly of higher order PSII complexes are affected in transgenic plants. We have discussed that $O_2^{\bullet-}$ originated from either Mehler's reaction or PSII itself may diffuse toward PSII reaction centers due to lack of FeSOD in transgenic plants and result in

conformational changes in the D1 protein around the Q_B binding site. Thus, it is reasonable to propose that active dimeric PSII complexes in transgenic plants tend to be instable even under normal light conditions, presumably due to conformational changes induced by $O_2^{\bullet-}$ attack, and then disassembled PSII migrates to stroma-exposed thylakoids followed by proteolytic degradation. Since assembly into functional PSII is included in the PSII repair steps [57] and transgenic plants are capable of repair from photoinhibition (Fig. 7B), it is unlikely that assembly of dimeric PSII and PSII-LHCII complexes are impaired in transgenic plants.

Indeed, the instability of PSII complex in transgenic plants was confirmed when exposed to high irradiance that enhances PSII photodamage. D1 and other PSII core proteins were degraded to a greater extent in high light in transgenic plants (Fig. 8). Additionally, we observed that $O_2^{\bullet-}$ levels increased with light intensity in both transgenic and WT plants, but its levels were constantly higher in transgenic plants than in WT plants (Fig. 9). Moreover, we did not observe the significant differences in the accumulation of $HO^{\bullet}$ and H_2O_2 between transgenic and WT plants during high light treatment. Thus, the instability of PSII complex under high light conditions in transgenic plants could result from high levels of $O_2^{\bullet-}$. We speculate that $O_2^{\bullet-}$ is more likely to induce the oxidation of amino acids in the D1 protein and other PSII core proteins and result in conformational changes which render the proteins susceptible to proteolytic degradation, as proposed earlier [58]. In addition, since other PSII core proteins are less oxidized than D1 [58,59], the extent of degradation of these proteins is lesser than that of D1.

It has been reported that ROS acts exclusively by inhibiting the repair of PSII and not by damaging PSII directly [9]. However, in this study, excess $O_2^{\bullet-}$ produced in transgenic plants induces photodamage to the PSII complex and increases D1 degradation but does not inhibit the repair process (Figs. 7 and 8). A possible explanation is that $O_2^{\bullet-}$ accumulated at high levels while H_2O_2 did not accumulate in transgenic plants (Fig. 3). $O_2^{\bullet-}$ and H_2O_2 may play different physiological roles in photoinhibition and they have different targets. In the model for the action of ROS in PSII repair, elongation factors appear to be the primary targets of H_2O_2 in cyanobacteria, and H_2O_2 might inhibit the synthesis de novo of the D1 protein by inactivating the elongation factors [7,9]. As for $O_2^{\bullet-}$, the possible target may be the D1 protein itself and other PSII proteins as discussed above.

In this study, we observed that decreased chloroplastic FeSOD resulted in a significant increase in the activity of chloroplastic Cu/ZnSOD when transgenic plants were grown under normal light conditions (100 μmol m^{-2} s^{-1}) (Table 3). However, we still observed an accumulation of $O_2^{\bullet-}$ in transgenic plants (Fig. 3A), indicating that the increased chloroplastic Cu/ZnSODs are not sufficient to detoxify accumulated $O_2^{\bullet-}$. Similar results were also observed in knockout FeSOD *Arabidopsis* plants [12]. It is thus suggested that an increase in the activity of chloroplastic Cu/ZnSOD could not compensate for the decreased FeSOD in transgenic plants.

It is generally believed that chloroplastic Cu/ZnSOD is attached to PSI [13,14], and appears to function as the first defense line to detoxify $O_2^{\bullet-}$ in the vicinity of PSI [14,50,60]. In this study, we observed that PSI is less affected in transgenic plants as compared to PSII (Fig. 6, Table 4). At the same time, there was a significant increase in the activity of chloroplastic Cu/ZnSODs in transgenic plants. Thus, our results suggest that an increase in the activities of chloroplastic Cu/ZnSODs may play an important role in detoxifying $O_2^{\bullet-}$ in the vicinity of PSI. Why an increase in the activity of Cu/ZnSODs in transgenic plants is not sufficient to detoxify $O_2^{\bullet-}$ especially when it is produced at the level of PSI? One possibility is that although $O_2^{\bullet-}$ is mainly produced around PSI, it can diffuse to the PSII reaction center along the membrane [51]. In addition, it is suggested that PSII contributes to the formation of $O_2^{\bullet-}$ at the acceptor side under limitation of electron transport reaction between PSII and PSI [21,53]. In this study, we observed that the PSII function is severely impaired and the amounts of PSII core proteins are significantly decreased in transgenic plants (Fig. 6). Our results suggest that the function of FeSOD may be associated with detoxifying $O_2^{\bullet-}$ originating from PSII itself and/or diffusing from PSI. Moreover, recent studies have shown that chloroplastic FeSOD (FSD2 and FSD3) act as ROS scavengers in the maintenance of early chloroplast development by protecting the chloroplast nucleoids from ROS by affecting the plastid-encoded gene expression [12]. In *fsd2* and *fsd3* single knockout mutants, chloroplast development in young seedlings is arrested and ROS is significantly increased. These mutants are highly sensitive to oxidative stress. The phenotypes of fsd2 and fsd3 could not be reversed by induction of chloroplastic Cu/ZnSOD. It has been shown that FSD3 is specifically located in the chloroplast nucleoids and that FSD3 and FSD2 form a hetero-complex in this region [12]. Chloroplastic Cu/ZnSOD is mainly located in the stromal face of the thylakoid membranes [13]. Thus, it is suggested that FeSOD and chloroplastic Cu/ZnSOD may have functional specialization within chloroplast due to their different localizations [12]. In this study, although the activity of chloroplastic Cu/ZnSOD increased significantly in transgenic plants, still there was an accumulation of $O_2^{\bullet-}$, which is possibly due to abnormal chloroplast development. Indeed, we observed that the chloroplasts of transgenic plants were smaller than that from the WT plants and their grana stacks were much less abundant (data not shown).

In conclusion, we obtained transgenic tobacco plants with severely decreased FeSOD in order to investigate the possible mechanisms of FeSOD in protection against photooxidative stress. Transgenic plants accumulated high levels of $O_2^{\bullet-}$ even under normal light conditions. Our results show that PSII was primarily affected in transgenic plants. Fluorescence relaxation and TL measurements suggested the acceptor side of PSII at the level of Q_A to Q_B electron transfer was significantly affected in transgenic plants. And immunoblot and blue native gel analyses indicated that the stability of PSII was affected in transgenic plants. The results in this study suggest that FeSOD plays an important role in maintaining PSII function by stabilizing PSII complexes in tobacco plants.

Acknowledgments

This study was supported by the National Natural Science Foundation of China (30971717) and the State Key Basic Research and Development Plan of China (2009CB118503). We are grateful to unknown reviewers for their valuable comments and constructive criticism that improved our manuscript.

References

[1] N. Adir, H. Zer, S. Shochat, I. Ohad, Photoinhibition—a historical perspective, Photosynth. Res. 76 (2003) 343–370.
[2] S.K. Sopory, B.M. Greenberg, R.A. Mehta, M. Edelman, A.K. Mattoo, Free radical scavengers inhibit light-dependent degradation of the 32 kDa photosystem II reaction center protein, Z. Naturforsch. 45c (1990) 412–417.
[3] G.X. Chen, J. Kazimir, G.M. Cheniae, Photoinhibition of hydroxylamine-extracted photosystem II membranes: studies of the mechanism, Biochemistry 31 (1992) 11072–11083.
[4] M. Miyao, Involvement of active oxygen species in degradation of the D1 protein under strong illumination in isolated subcomplexes of photosystem II, Biochemistry 33 (1994) 9722–9730.
[5] M. Miyao, M. Ikeuchi, N. Yamamoto, T. Ono, Specific degradation of the D1 protein of photosystem II by treatment with hydrogen peroxide in darkness: implication for the mechanism of degradation of the D1 protein under illumination, Biochemistry 34 (1995) 10019–10026.
[6] K. Okada, M. Ikeuchi, N. Yamamoto, T. Ono, M. Miyao, Selective and specific cleavage of the D1 and D2 proteins of photosystem II by exposure to singlet oxygen: factors responsible for the susceptibility to cleavage of the proteins, Biochim. Biophys. Acta 1274 (1996) 73–79.
[7] Y. Nishiyama, H. Yamamoto, S.I. Allakhverdiev, H. Inaba, A. Yokota, N. Murata, Oxidative stress inhibits the repair of photodamage to the photosynthetic machinery, EMBO J. 20 (2001) 5587–5594.

[8] Y. Nishiyama, S.I. Allakhverdiev, H. Yamamoto, H. Hayashi, Singlet oxygen inhibits the repair of photosystem II by suppressing the translation elongation of the D1 protein in *Synechocystis* sp. PCC 6803, Biochemistry 43 (2004) 11321–11330.
[9] Y. Nishiyama, S.I. Allakhverdiev, N. Murata, A new paradigm for the action of reactive oxygen species in the photoinhibition of photosystem II, Biochim. Biophys. Acta 1757 (2006) 742–749.
[10] C. Bowler, M. Van-Montagu, D. Inzé, Superoxide dismutase and stress tolerance, Annu. Rev. Plant Physiol. Plant Mol. Biol. 43 (1992) 83–116.
[11] R.G. Alscher, N. Erturk, L.S. Heath, Role of superoxide dismutases (SODs) in controlling oxidative stress in plants, J. Exp. Bot. 53 (2002) 1331–1341.
[12] F. Myouga, C. Hosoda, T. Umezawa, H. Lizumi, T. Kuromori, R. Motohashi, Y. Shono, N. Nagata, M. Lkeuchi, K. Shinozaki, A heterocomplex of iron superoxide dismutases defends chloroplast nucleoids against oxidative stress and is essential for chloroplast development in *Arabidopsis*, Plant Cell 20 (2008) 3148–3162.
[13] K. Ogawa, S. Kanematsu, K. Takabe, S. Asada, Attachment of CuZn-superoxide dismutase to thylakoid membranes at the site of superoxide generation (PSI) in spinach chloroplasts: detection by immunogold labeling after rapid freezing and substitution method, Plant Cell Physiol. 36 (1995) 565–573.
[14] K. Asada, The water–water cycle in chloroplasts: scavenging active oxygen species and dissipation of excess photons, Annu. Rev. Plant Physiol. Mol. Biol. 50 (1999) 601–639.
[15] W. Van Camp, K. Capiau, M. Van-Montagu, D. Inzé, L. Slooten, Enhancement of oxidative stress tolerance in transgenic tobacco plants overproducing Fe-superoxide dismutase in chloroplasts, Plant Physiol. 112 (1996) 1703–1714.
[16] F. Navari-Izzo, M.F. Quartacci, C. Pinzino, F. Dalla Vecchia, C.L.M. Sgherri, Thylakoid-bound and stromal enzymes in wheat treated with excess copper, Physiol. Plant. 104 (1998) 630–638.
[17] T. Pfannschmidt, K. Ogrzewalla, S. Baginsky, A. Sickmann, H.E. Meyer, G. Link, The multisubunit chloroplast RNA polymerase A from mustard (*Sinapis alba* L.). Integration of a prokaryotic core into a larger complex with organelle-specific functions, Eur. J. Biochem. 267 (2000) 253–261.
[18] J. Pfalz, K. Liere, A. Kandlbinder, K.J. Dietz, R. Oelmüller, pTAC2, -6, and -12 are components of the transcriptionally active plastid chromosome that are required for plastid gene expression, Plant Cell 18 (2006) 176–197.
[19] B.K. Phee, J.H. Cho, S. Park, J.H. Jung, Y.H. Lee, J.S. Jeon, S.H. Bhoo, T.R. Hahn, Proteomic analysis of the response of *Arabidopsis* chloroplast proteins to high light stress, Proteomics 4 (2004) 3560–3568.
[20] E. Tyystjärvi, M. Riikonen, M. A-C, R. Kettunen Arisi, L. Jouanin, C.H. Foyer, Photoinhibition of photosystem II in tobacco plants overexpressing glutathione reductase and poplars overexpressing superoxide dismutase, Physiol. Plant. 105 (1999) 409–416.
[21] P. Pospíšil, A. Arato, A. Krieger-Liszkay, A.W. Rutherford, Hydroxyl radical generation by photosystem II, Biochemistry 43 (2004) 6783–6792.
[22] A. Tiwari, P. Pospíšil, Superoxide oxidase and reductase activity of cytochrome b_{559} in photosystem II, Biochim. Biophys. Acta 1787 (2009) 985–994.
[23] S.V. Wesley, C.A. Helliwell, N.A. Smith, M.B. Wang, D.T. Rouse, Q. Liu, P.S. Goodin, S. P. Singh, D. Abbott, P.A. Stoutjesdijk, S.P. Robinson, A.P. Gleave, A.G. Green, P.M. Waterhouse, Construct design for efficient, effective and high-throughput gene silencing in plants, Plant J. 27 (2001) 581–590.
[24] G. An, Binary Ti vectors for plant transformation and promoter analysis, Meth. Enzymol. 153 (1987) 292–305.
[25] R.B. Horsh, J.E. Fry, H.L. Hoffman, D. Eicholts, S.G. Rogers, R.T. Fraley, Simple and general method for transferring genes into plants, Science 277 (1985) 1229–1231.
[26] S. Ding, Q. Lu, Y. Zhang, Z. Yang, X. Wen, L. Zhang, C. Lu, Enhanced sensitivity to oxidative stress in transgenic tobacco plants with decreased glutathione reductase activity leads to a decrease in ascorbate pool and ascorbate redox state, Plant Mol. Biol. 69 (2009) 577–592.
[27] J. Kurepa, D. Herouart, M. Van-Montagu, Differential expression of CuZn- and Fe-superoxide dismutase genes of tobacco during development, oxidative stress, and hormonal treatments, Plant Cell Physiol. 38 (1997) 463–470.
[28] M. Kawai-Yamada, Y. Ohori, H. Uchimiya, Dissection of *Arabidopsis* Bax inhibitor-1 suppressing Bax-, hydrogen peroxide-, and salicylic acid-induced cell death, Plant Cell 16 (2004) 21–32.
[29] H. Thordal-Christensen, Z. Zhang, Y. Wei, D.B. Collinge, Subcellular localization of H_2O_2 in plants: H_2O_2 accumulation in papillae and hypersensitive response during the barley–powdery mildew interaction, Plant J. 11 (1997) 1187–1194.
[30] S. Veljovic-Jovanovic, G. Noctor, C.H. Foyer, Are leaf hydrogen peroxide concentrations commonly overestimated? The potential influence of artefactual interference by tissue phenolics and ascorbate, Plant Physiol. Biochem. 40 (2002) 501–507.
[31] A. Ros-Barceló, The generation of H_2O_2 in the xylem of Zinnia elegans is mediated by an NADPH-oxidase-like enzyme, Planta 207 (1998) 207–216.
[32] K. Yoshimura, K. Miyao, A. Gaber, T. Takeda, H. Kanaboshi, H. Miyasaka, S. Shigeoka, Enhancement of stress tolerance in transgenic tobacco plants over-expressing *Chlamydomonas* glutathione peroxidase in chloroplasts or cytosol, Plant J. 37 (2004) 21–33.
[33] J. Meurer, K. Meierhoff, P. Westhoff, Isolation of high chlorophyll-fluorescence mutants of *Arabidopsis thaliana* and their characterization by spectroscopy, immunoblotting and northern hybridization, Planta 198 (1996) 385–396.
[34] L. Peng, J. Ma, W. Chi, J. Guo, S. Zhu, Q. Lu, C. Lu, L. Zhang, Low PSII Accumulation1 is involved in efficient assembly of photosystem II in *Arabidopsis thaliana*, Plant Cell 18 (2006) 955–969.
[35] H.K. Laemmli, Cleavage of structural proteins during the assembly of the head of bacteriophage T4, Nature 227 (1970) 680–685.
[36] D.I. Arnon, Copper enzymes in isolated chloroplasts. Polyphenoloxidase in *Beta vulgaris*, Plant Physiol. 24 (1949) 1–15.
[37] M.M. Bradford, A rapid and sensitive method for the quantification of microgram quantities of protein using the principal of protein–dye binding, Anal. Biochem. 72 (1976) 248–254.
[38] I. Šnyrychová, F. Ayaydin, É. Hideg, Detecting hydrogen peroxide in leaves in vivo —a comparison of methods, Physiol. Plant. 135 (2009) 1–18.
[39] K. Schult, K. Meierhoff, S. Paradies, T. Töller, P. Wolff, P. Westhoff, The nuclear-encoded factor HCF173 is involved in the initiation of translation of the psbA mRNA in *Arabidopsis thaliana*, Plant Cell 19 (2007) 1329–1346.
[40] I. Vass, E. Turcsanyi, E. Touloupakis, D. Ghanotakis, V. Petrouleas, The mechanism of UV-A radiation-induced inhibition of photosystem II electron transport studied by EPR and chlorophyll fluorescence, Biochem. 41 (2002) 10200–10208.
[41] I. Vass, Govindjee, Thermoluminescence from the photosynthetic apparatus, Photosynth. Res. 48 (1996) 117–126.
[42] Y. Inoue, Photosynthetic thermoluminescence as a simple probe of photosystem II electron transport, in: J. Amesz, J. Hoff (Eds.), Biophysical Techniques in Photosynthesis, Advances in Photosynthesis vol. 3, Kluwer Academic Publishers, Dordrecht, 1996, pp. 93–107.
[43] I. Vass, G. Horvath, T. Herczeg, S. Demeter, Photosynthetic energy conservation investigated by thermoluminescence. Activation energies and half-lives of thermoluminescence bands of chloroplasts determined by mathematical resolution of glow curves, Biochim. Biophys. Acta 634 (1981) 140–152.
[44] A.W. Rutherford, A.R. Crofts, Y. Inoue, Thermoluminescence as a probe of photosystem II photochemistry: the origin of the flash-induced glow peaks, Biochim. Biophys. Acta 682 (1982) 457–465.
[45] S. Demeter, I. Vass, Charge accumulation and recombination in photosystem II studied by thermoluminescence: I. Participation of the primary acceptor Q and secondary acceptor B in the generation of thermoluminescence of chloroplasts, Biochim. Biophys. Acta 764 (1984) 24–32.
[46] J.-M. Ducreut, I. Vass, Thermoluminescence: experimental, Photosynth. Res. 101 (2009) 195–204.
[47] J. Guo, Z. Zhang, Y. Bi, W. Yang, Y. Xu, L. Zhang, Decreased stability of photosystem I in *dgd1* mutant of *Arabidopsis thaliana*, FEBS Lett. 579 (2005) 3619–3624.
[48] A.K. Mattoo, H. Hoffman-Falk, J.B. Marder, M. Edelman, Regulation of protein metabolism: coupling of photosynthetic electron transport to in vivo degradation of the rapidly metabolized 32-kilodalton protein of the chloroplast membranes, Proc. Natl Acad. Sci. USA 81 (1984) 1380–1384.
[49] S.K. Herbert, G. Samson, D.C. Fork, D.E. Laudenbach, Characterization of damage to photosystems I and II in a cyanobacterium lacking detectable iron superoxide dismutase activity, Proc. Natl Acad. Sci. USA 89 (1992) 8716–8720.
[50] K. Asada, Production and scavenging of reactive oxygen species in chloroplasts and their functions, Plant Physiol. 141 (2006) 391–396.
[51] L. Slooten, K. Capiau, W. Van Camp, M. Van-Montagu, C. Sybesma, D. Inzé, Factors affecting the enhancement of oxidative stress tolerance in transgenic tobacco overexpressing manganese superoxide dismutase in the chloroplasts, Plant Physiol. 107 (1995) 737–750.
[52] P. Pospíšil, I. Snyrychova, J. Kruk, K. Strzalka, J. Naus, Evidence that cytochrome b559 is involved in superoxide production in photosystem II: effect of synthetic short-chain plastoquinones in a cytochrome b559 tobacco mutant, Biochem. J. 397 (2006) 321–327.
[53] P. Pospíšil, Production of reactive oxygen species by photosystem II, Biochim. Biophys. Acta 1787 (2009) 1151–1160.
[54] B. Loll, J. Kern, W. Saenger, A. Zouni, J. Biesiadka, Towards complete cofactor arrangement in the 3.0 A resolution structure of photosystem II, Nature 438 (2005) 1040–1044.
[55] A.W. Rutherford, Govindjee, Y. Inoue, Charge accumulation and photochemistry in leaves studied by thermoluminescence and delayed light emission, Proc. Natl Acad. Sci. USA 81 (1984) 1107–1111.
[56] Y.G. Song, B. Liu, L.F. Wang, M.H. Li, Y. Liu, Damage to the oxygen-evolving complex by superoxide anion, hydrogen peroxide, and hydroxyl radical in photoinhibition of photosystem II, Photosynth. Res. 90 (2006) 67–78.
[57] E.M. Aro, M. Suorsa, A. Rokka, Y. Allahverdiyeva, V. Paakkarinen, A. Saleem, N. Battchikova, E. Rintamaki, Dynamics of photosystem II: a proteomic approach to thylakoid protein complexes, J. Exp. Bot. 56 (2005) 347–356.
[58] E. Kapri-Pardes, L. Naveh, Z. Adam, The thylakoid lumen protease Deg1 is involved in the repair of photosystem II from photoinhibition in *Arabidopsis*, Plant Cell 19 (2007) 1039–1047.
[59] J. Sharma, M. Panico, C.A. Shipton, F. Nilsson, H.R. Morris, J. Barber, Primary structure characterization of the photosystem II D1 and D2 subunits, J. Biol. Chem. 272 (1997) 33158–33166.
[60] S.M. Choi, S.W. Jeong, W.J. Jeong, S.Y. Kwon, W.S. Chow, Y.-I. Park, Chloroplast Cu/Zn-superoxide dismutase is a highly sensitive site in cucumber leaves chilled in the light, Planta 216 (2002) 315–324.